Design and Optimization of a Three-Dimensional   Small Wind-Tunnel Contraction Section

Aqeel Ashoor Abd
aqeelashoor3@gmail.com
Engineering College
Baghdad University\Iraq
Dr. Anmar H. Ali
lecturer
aha_has@yahoo.com

Abstract:- In this article, A contraction has been designed, manufactured at the Mechanical Engineering Department at Baghdad University - College of Engineering. The theoretical study was accomplished by **ANSYS workbench 15.0** and using к-ε turbulence model to simulate turbulent flow in a 3-D contraction section of small low subsonic wind tunnel. A sixth-order polynomial equation had been adopted with a specified boundary conditions to represent a smooth contraction wall profile shape. Seven inflection points are chosen to give seven different contractions. An experimental low-speed wind tunnel of test cross section area $(0.45 \times 0.45 \ m^2)$ and new contraction section was built and tested for maximum velocity at test section 20 m/s. Boundary layer thickness, static pressure and secondary flow and the maximum uniformity are considered as optimization parameters. Numerical results show that boundary layer thickness decreases, variation in wall normal velocity components at the test section inlet increases, and probability of flow separation increases as the inflection point moves towards the contraction outlet. The optimized contraction is investigated computationally and experimentally. The experimental results of contraction compared well with the computational code **ANSYS workbench 15.0** results.
Keywords: design of contraction section, small wind tunnel, test section, contraction ratio, optimization of contraction section.

1. Introduction

The aerodynamics is largely dependent on experimental science observations, so the wind tunnel can be considered as an important tool for the aerodynamic design of aircraft, turbomachines, cars,...etc. The Optimum wind–tunnel design is characterized by a maximum air flow rate, and best flow quality at a minimum power consumption, dimension, and the cost of construction. The flow quality is

based on many parameters such as contraction wall profile, contraction ratio, number of screens and type of honeycomb. The contraction is the most important portion of the low speed wind-tunnel. The function of the proper design of the contraction, is to give a steady flow with uniform velocity distribution at the inlet of the test section. It get the flow from the screen and honeycomb(settling chamber) to the test section when increasing the average speed[1]. The profile of the contraction walls has of a great action on the velocity uniformity of the test section. There is an important principle in the contraction design for low-speed wind-tunnel(LSWT). These principles are to make the contraction as short as possible with optimum performance. An important parameter for a better contraction design is the contraction ratio (CR). The most important advantage of this parameter is to give the required velocity at the test section and give a low speed in the settling chamber. This low speed helps to use more than one screen and a fine honeycomb without excessive power loss [2]There are two main types of contraction which are straight and concave- convex shapes, the polynomial equation that represent contraction profile or two elliptic to draw the curve of contraction. The main advantage of the contraction are to minimize the mean and fluctuating velocity differences. The contraction consists of two main sections; [i] concave shape and it is most important to avoid the occurrence of separation of boundary layer. [ii] convex walls that may reason flow separation in the neighborhood of the contraction outlet(test section inlet) due to a positive pressure gradient [3] LSWT contraction section design with maximum flow uniformity at the test section, without separation, minimizing the boundary layer thickness at the test section exit, no Gortler vortices in the contraction and the turbulence level were considered to optimize the contraction profile which was based on the delineation method[4]. The present work aims to provide a design procedure for the contraction section of a small LSWT with the maximum velocity uniformity at the exit plane of the contraction, no separation, and small boundary layer thickness at the entrance of the test section which are the main objectives to optimize the contraction geometry.

2- The Contraction Geometry and Coordinate System
2.1 Coordinate System

A three-dimensional square to square contraction model is shown in **Fig. 1.**

1m

1.1m

0.45m

0.45m

(a)

1m

0.45m
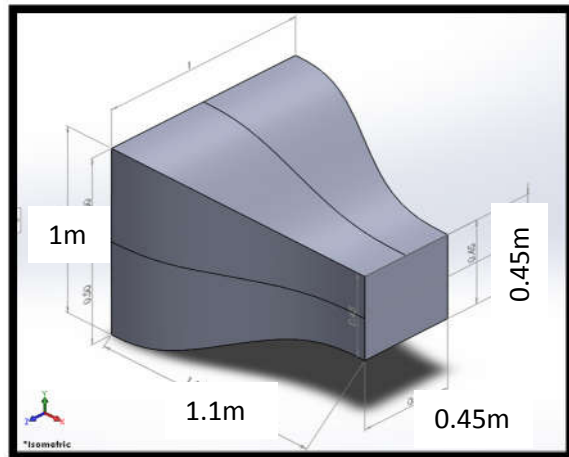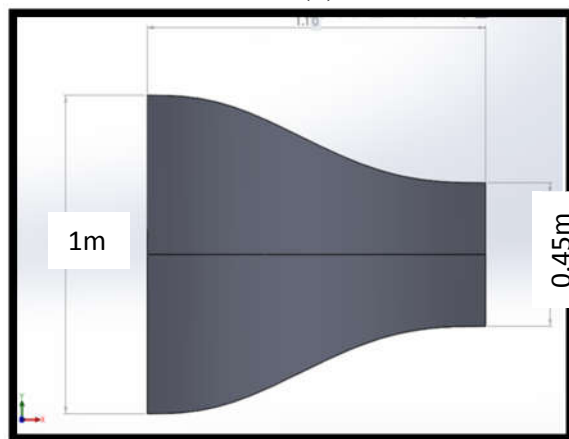
(b)

Fig.1 The Three-Dimensional Square To Square Contraction Model, (a)Isometric View (b)Side View

The contraction geometry is represented by a three-dimensional Cartesian-coordinates X,Y,Z, where the length of contraction is along X-axis, the height of the contraction is along Y-axis and the width of contraction is along Z-axis. Due to similarity, a quarter geometry was used to reduce numerical solution memory and consuming time as shown in Figure 2.

0.5m

0.5m

1.1m

0.225m
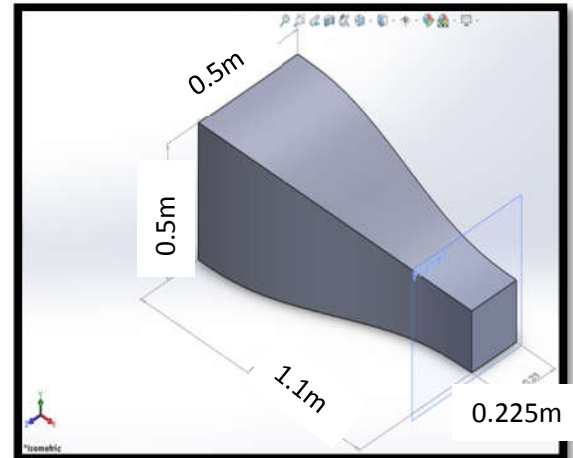
Fig.2 The Three-Dimensional One Quarter Of The Square To Square Contraction

2.2 The Contraction Basic Sizes

The square section of the test section is (0.45m×0.45m) and the flow maximum velocity is equal to v=20m/s. So that, the contraction outlet height and width are (0.45m, 0.45m). Assuming the Contraction ratio equal to (CR=5), where CR=$\frac{A_i}{A_o}$, the Bradshaw and Mehta showed the best Contraction ratio is between (5 to 9). Where A_i: represented the contraction inlet area ($1m^2$), and A_o: represented the contraction outlet area($0.2025m^2$). The contraction inlet height and width are (1m). The contraction length is 1.1m as Downie and jordinson assumed that the Contraction length approximately equal to the Contraction inlet height.

2.3 Contraction Wall Profile

A six order polynomial equation has been chosen to represent the contraction profile. Inflection point must be determined to make the contraction profile with concave and convex shape. The equation consists of seven constants as in equation(1).

$$Y = ax^6 + bx^5 + cx^4 + dx^3 + ex^2 + fx + g$$
.... (1)

Where a, b, c, d, e, f and g are the constants of the polynomial equation which are evaluated using seventh boundary conditions to find the final equation of the contraction profile geometry. These boundary conditions are illustrated clearly by Ahmed and eljack as follows:

1. The contraction entrance $x = 0$ m
$\frac{H_i}{2}$ =0.5

2. The contraction exit x =1.1 m
$\frac{H_o}{2}$ =0.225

3. At the contraction entrance (The slope of profile equals zero to make the wall parallel to the flow):
$\frac{dy}{dx}$=0 $x = 0$ m

4. At the contraction exit (The slope of profile equals zero to make the wall parallel to the flow):
$\frac{dy}{dx}$=0   x=1.1 m

5. At the contraction entrance:
$\frac{dy^2}{dx^2} = 0$ x=0 m

6. At the contraction exit: :
$\frac{dy^2}{dx^2} = 0$ x = 1.1 m

7. The seventh condition was the position of inflection point is assumed

to vary as follows; x= 0.3,0.45, 0.475, 0.5, 0.55, 0.6, 0.65, 0.7 and 0.8. The boundary conditions were applied in the equation(1) to find the following set of equations: g=0.5, f=0, e=0
The set of equations can be represented as follows;

$$\begin{bmatrix} x^6 & x^5 & x^4 & x^3 \\ 6x^5 & 5x^4 & 4x^3 & 3x^2 \\ 30x^4 & 20x^3 & 12x^2 & 6x \\ 30x^4 & 20x^3 & 12x^2 & 6x \end{bmatrix} \times \begin{bmatrix} a \\ b \\ c \\ d \end{bmatrix} = \begin{bmatrix} -0.275 \\ 0 \\ 0 \\ 0 \end{bmatrix}$$

3- Numerical Solution
3.1 Assumptions
The following assumptions which are used in the present work are;
1. Steady flow.
2. Three-dimensional flow.
3. Subsonic incompressible flow, (M ≤ 0.3).
4. Neglecting gravity force.
5. Newtonian continuom flow.
6.Turbulent flow through the contraction.
7. No heat transfer is considered.
3.2 The Governing Equations
The flow is governed by the following equations;

(i) Continuity Equation

$$\frac{\partial}{\partial x_i} u_i = 0 \qquad \text{.....................} (2)$$

(ii) Momentum Equations

$$u_j \frac{\partial u_i}{\partial x_j} = -\frac{1}{\rho}\frac{\partial P}{\partial x_i} + \frac{\partial}{\partial x_j}(\vartheta \frac{\partial u_i}{\partial x_j} - u_i u_j)$$
.... (3)

(iii) K-ε (turbulence model)

K-ε turbulence model is the most common model which is used in computational fluid dynamic (CFD) to simulate mean flow characteristics for turbulent flow conditions. The exact K-ε equations contain many unknown and immeasurable terms of a much more practical approach.

(iii) Boundary Condition

Assuming the exit plane of contraction with atmospheric zero pressure and the inlet dynamic pressure of the test section as inlet of contraction pressure. This condition gives accurate simulation to the contraction.

-Inlet boundary condition: from the dynamic pressure equation for the test section which is $(p=\frac{1}{2}\rho v^2)$, where: $v = 20m/s$(maximum velocity) and $\rho = 1.225\ kg/m^3$ then the pressure at inlet contraction became (P_i=245 pa).Turblenec intensity taken as 2.5%.

-No slip condition: the relative velocity components between flow and wall of contraction are equal to zero.

-Outlet boundary condition: the pressure at the outlet of the contraction equal atmosphere (P_o=0 pa).

-Symmetrical boundary condition: Two planes of contraction geometry are symmetrical as shown in **Fig. 3**

shows the contraction geometry with previous boundary conditions.
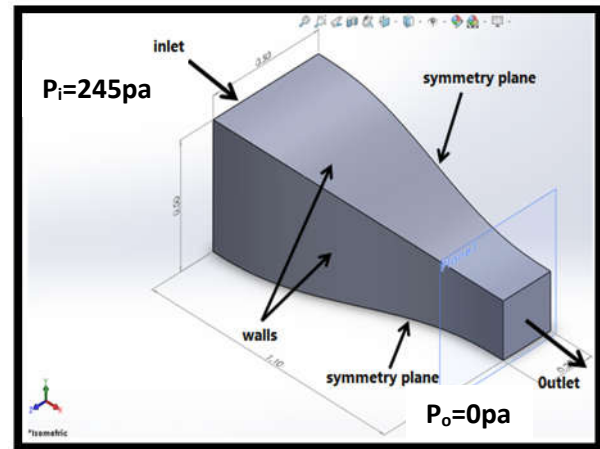
Fig.3 The Three Dimensional Contraction Shape With Boundary Conditions.

3.3 Grid Generation

A mesh is defined by dividing the model's geometry into simple shapes of small units.. A free mesh has been used to define the geometry in the present work. Because of the uniformity of the geometry in the free mesh defines the computational domain automatically by mapped discretization as shown in the **Fig.4**.

Fig.4 Mesh Of Domain The Contraction Model,(Isometric View)

The required high quality meshes must be used to accurately capture the complex physical phenomena, but it is computationally expensive. Therefore, the selection number of elements is based on the grid independence test. The total number of grid elements is about 131328 as shown in the grid independence test between the static pressure at center line and the number of cells as shown in **Fig. 5**.

Fig.5 Grid Independence Test

4- Experimental Work

4.1 The Wind Tunnel

The present LSWT shown in Figure 6 consists of the following parts:

Fig.6 The Open Circuit Wind Tunnel

- Bell Mouth; which is used to increase the area of inlet section and to prevent separation of flow at the edge of the inlet section as shown in **Fig.7**.

Fig.7 The Bell Mouth

- Settling chamber; this section is important to damp out the turbulence of flow by using honeycombs and

grids are chosen in this section. Square cross-section of settling chamber was made of steel sheet and connected with a bell mouth as one unit as shown in **Fig.8**.
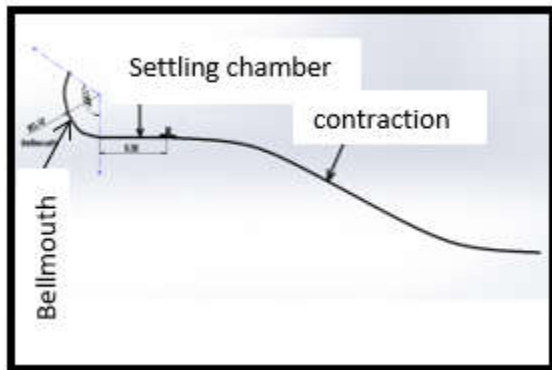
Fig.8 The Bellmouth, Settling Chamber And Contraction Where Constructed As One Unit

- Contraction section; Which was made of steel sheets and have a square cross-section. Also, the contraction ratio =5 where inlet area is (0.1x0.1 m^2) and exit area equal to (0.45x0.45 m^2).
- Test section; The test section was reconstructed of (0.01m) wood thickness cross section and the length(0.75m),square shape(0.45m× 0.45m).
- Diffuser ; The diffuser is used to link the fan casing (exit diffuser diameter =75cm and the length of diffuser is 1.5m)with the test section(square area shape (0.45mx0.45m)) and converting the cross sectional area from the square shape to circular, the divergence angle are(7.6˚).

- The fan house; the motor of the fan electric coil was replaced to increase the rotation speed from 1400 rpm to 3000 rpm with horse power 1hp.

4.2 The manufacture contraction
The experiments are used on the square to square contraction.The current contraction is made of four stainless steel plate sections, that are cut off exactly by using (CNC machine) with full size as shown in **Fig. 9**.

Fig.9 The square to square contraction

4.3 Measurements and Instrumentations
i- The Static Pressure Taps
The contraction was tubed from the left and top side with nine holes in each side (the inner diameter of the hole=4mm) to measure the static pressure, as shown in the Figure 10. Also, The test section was drilled with seven taps from two sides, for the testing the uniformity of flow(the diameter of hole =8mm).
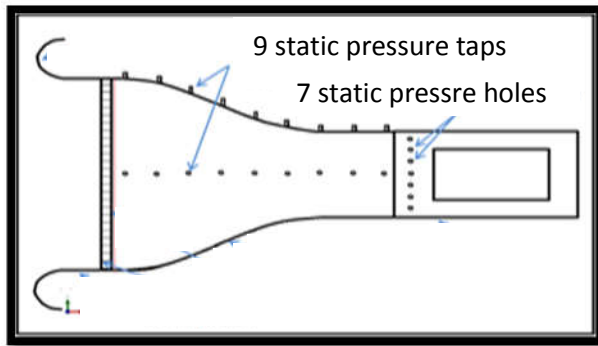
Fig.10 The Sketch Of Settling Chamber, Contraction And The Test Section

ii- The Static Pressure Tube

A stainless steel tube with 4mm inner diameter and the length 1.5m with closed end of one side, as shown in **Fig.11**.
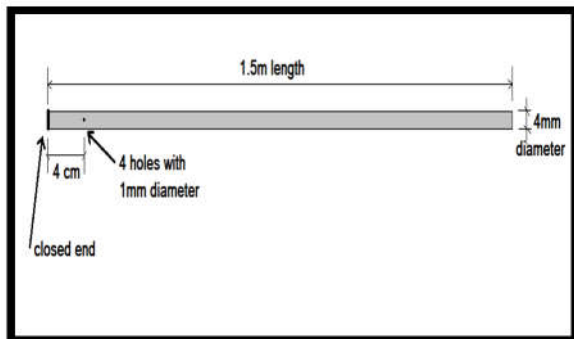
Fig.11 The Static Pressure Tube

iii- The Pitot - Static Tube

The most common device to determine the total head and the static, dynamic and total pressure of a flow in the test section of the open wind tunnel is the pitot-static tube.

iv- The Micro-Manometer

A digital manometer is used to read differential pressure. It consists of a digital screen with a button on and off and a button to convert pressure units. The device was calibrated by the Iraq Organization for calibration. The device calibration shows 1.5% error reading.

5. Results and Discussions

5-1 Numerical Results

The flow properties (static pressure, uniformity, shear stresses, boundary layer thickness, velocity profiles of boundary layer... etc.) was calculated for the contraction section and verified with the experimental data. The contraction profiles are illustrated and presented in **Fig. 12**
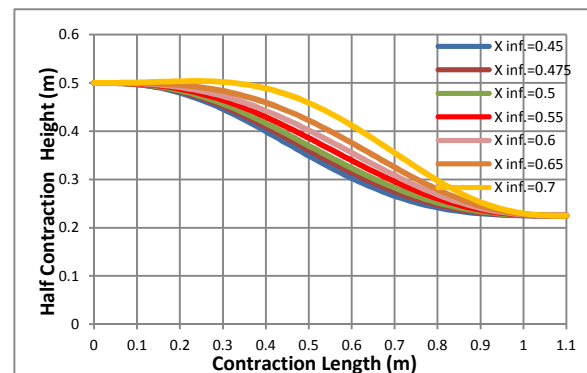
Fig.12 The Contraction Wall Profiles

Seven inflection points are considered for the present three dimensional contraction profile as shown in **Fig. 13.**
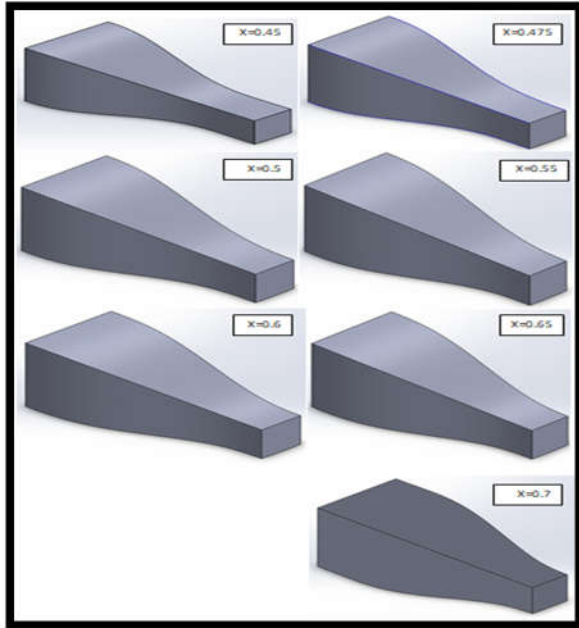
Fig.13 Three-Dimension Contraction Sections for Seven Inflection Points

Figure 14 shows the velocity at the center line for the present contractions. This figure shows that the velocity is about (4m/s) which is increased from a minimum value at contraction to the maximum (20m/s), because of the effects of wall contraction shape. The growth of the boundary layer thickness with the profile shape of the contraction leads to reduce the contraction area at the outlet and that may increase the velocity causing these differences between them at the contraction outlet as shown in the figure. The flow inlet

velocity 4m/s at the entrance of the settling chamber is used to decrease the losses and accelerated to the required velocity at the test section which is 20m/s . It may be noted that the profiles $X_{inf.}=0.55$ and $X_{inf.}=0.6$ have the highest velocities(about V=22.8m/s)as shown in **Fig.14 .**
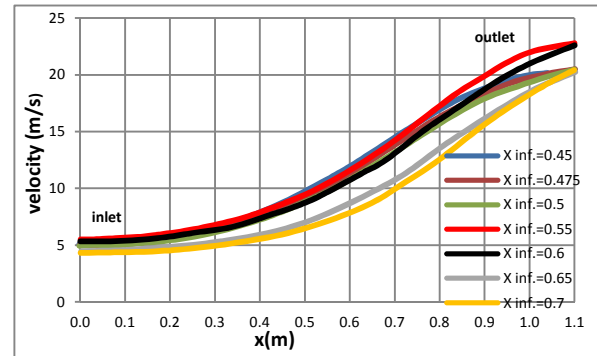
Fig.14 Velocity at The Center Line for Contractions

Fig. 15 shows the pressure at corner, side, top walls and center line for the inflection points $X_{inf.}=0.55$ From this figure, it may be seen that the top and side wall pressures for different contraction sections are symmetric from the inlet section to outlet along the contraction length. The corner pressure is different from the other due to intraction between the top and side walls Boundary layer which causes this defect in pressure as compared with others. A new curve has been created at the corner line causing these defects. No overshoots data are noticed near the inlet section

as shown in figure due to smooth transit profile.
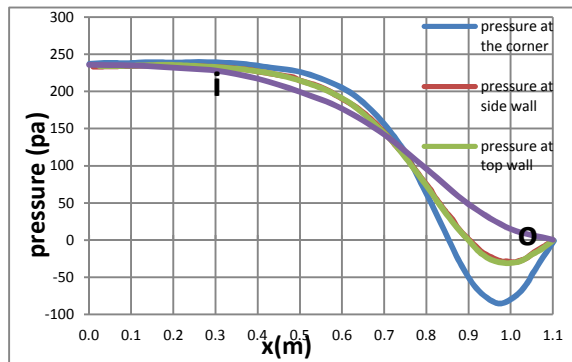
Fig.15 The Pressure at Corner, Side, Top Walls and Center Line For Inflection Point $X_{inf.}=0.55$

Figure 16 shows the shear stress at corner, side and top walls for inflection points $X_{inf.}=0.55$. The shear stress has been increased from the entrance of the contraction to the exit section due to the effects of increasing the gradient of the velocity at the wall and flow momentum until it reaches the highest value, then it begins to decrease at the exit of the contraction because the increasing of boundary layer thickness and increasing the velocity at this region.
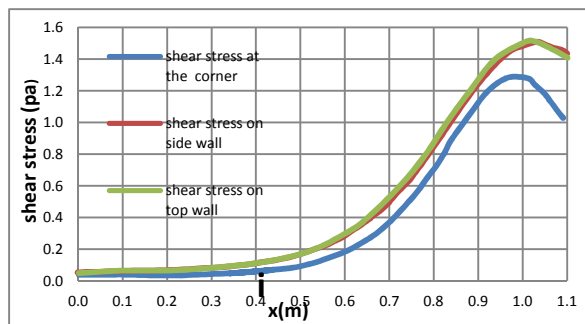
Fig.16 Shear Stress at Corner ,Side and Top Walls For Inflection Point $X_{inf.}=0.55$

The **Fig. 17** shows the Boundary layer velocity profiles planes at the test section inlet. The seven position contraction profiles were considered to find the velocity profiles throughout the contraction length. From these results, the thinner boundary layer occurs when the inflection point moves to exit section of the contraction.
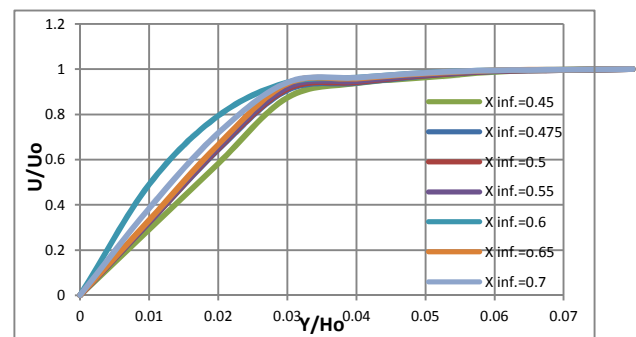
Fig.17 Boundary Layer velocity Profiles At Test Section Inlet

Fig. 18 shows the secondary flow(y-velocity) in exit plane of the contraction section. From this figure, it can be observed that the variation in V and W velocities at the test section inlet is a result of the growing the boundary layer, which works to push the flow towards contraction. This is cleared in the profile number one ($X_{inf.=}0.45$), then it increased from the contraction profile $X_{inf.=}0.475$ to $X_{inf.=}0.7$ respectively. For seven contraction profiles, Z-direction velocity have the same velocity profiles.
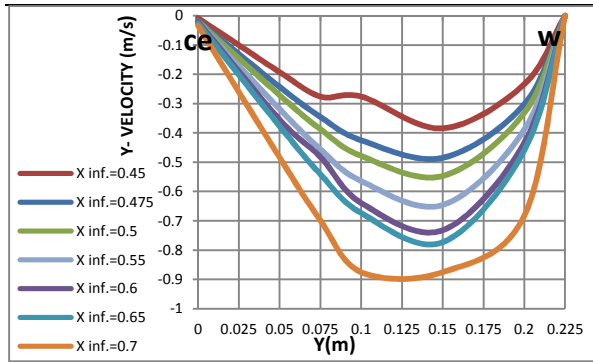
Fig.18 The Y-Velocity in Exit Plane at The Test Section Inlet

Fig. 19 shows the uniformity parameters with the inflection points. From this figure, it can be observed that the maximum uniformity at the inflection points between the $X_{inf.}=0.55$ and $X_{inf.}=0.6$.
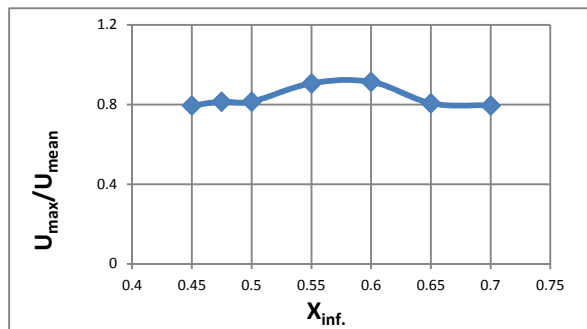
Fig.19 Uniformity With Inflection Points

Figure 20 shows the flow velocity contour for the inflection point $X_{inf.}=0.55$. From this figure, it can be observed that the red color contours represent the high velocity regions at the exit of the contraction(test section inlet) and the blue color regions represent the low velocity contours at the entrance of the contraction. The

boundary layer region is clear from this figure at wall of the contraction positions.
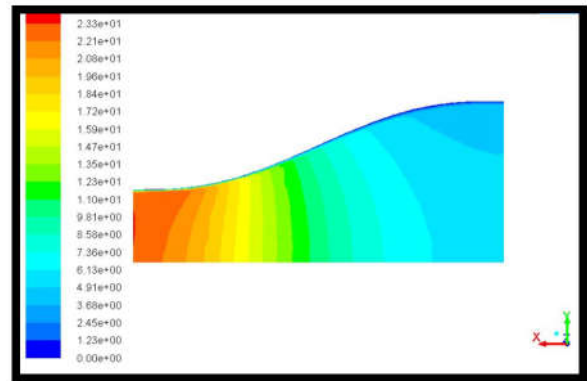
Fig.20 The Flow Velocity Contours For $X_{inf.}=0.55$

Fig. 21 shows the pressure contours for inflection point $X_{inf.}=0.55$. From this figure, it can be observed that the pressure distribution inside the contraction section. High pressure (red color) is found at the inlet section of the contraction while low pressure (blue color) at the exit of the contraction (test section inlet).
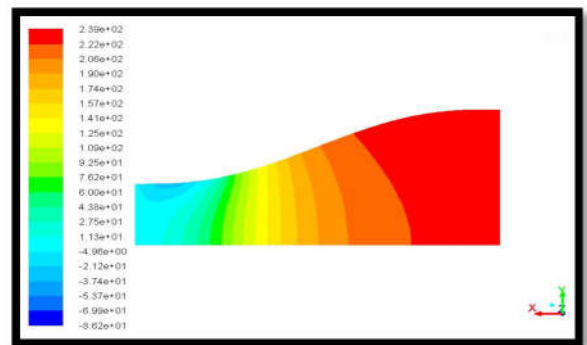
Fig.21 The Flow Pressure Contours For $X_{inf.}=0.55$

5-2 Best Contraction Profile

The numerical results indicated that of these criteria, the contraction profile number four ($X_{inf.}$=0.55) represents the thinner boundary layer thickness. The contraction profile number one ($X_{inf.}$=0.475) represents the best decreasing in the static pressure drop. The contraction profile number one ($X_{inf.}$=0.45) represents the best decreasing in the normal velocities at the test section inlet. The maximum uniformity was found at the inflection point the $X_{inf.}$=0.55,also, it can be observed the minimum uniformity is obtained at the $X_{inf.}$=0.45. Based on previous results the contraction profile number four ($X_{inf.}$0.55), in which the inflection point is located at the middle of the contraction axis, was chosen to be the best profile for this wind-tunnel.were chosen to be the best profile.

5-3 Experimental Results

In this work, based on theoretical results by choice ($X_{inf.}$0.55) the best profile, experimental results are represented by four tests. The static pressure along the contraction section surface(side and top walls) were measured by wall taps. The uniform velocity in the test section was calculated by measuring the dynamic pressure at the test section inlet from seven holes on the two sides of the test section using pitot static tube. The pressure distributions on the center line of the contraction was measured by using the static pressure tube along the contraction center axis.The maximum velocity recorded during this investigation is about (20 m/s).

5.3 Comparison of Theoretical and Experimental Results

The four experimental tests with speed (20m/s) will be used as a data for comparison with the theoretical **ANSYS Workbench 15.0,**to compare the experimental pressure with the theoretical results, the minumm value of experimental pressure which is indicated at the inlet test section had been subtracted from the atmospheric pressure at the inlet of contraction.The theoretical pressure distribution along center line of the contraction, the pressure distribution on the side and top walls and the uniform velocity at the test section are in good agreement with the contraction experimental results, as shown in **Figures 22, 23, and 24.**
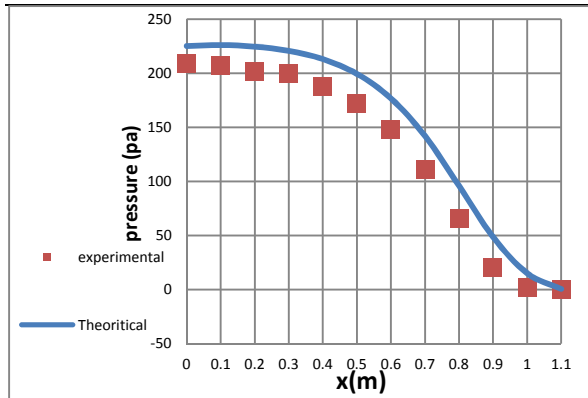
Fig.23 Comparison of Theoretical and Experimental Pressure at Center Line of Contraction
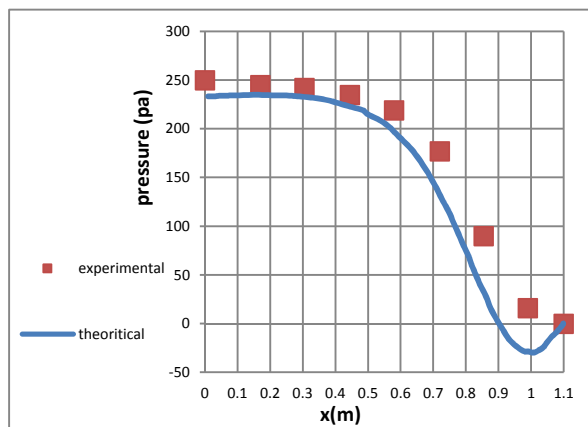
Fig.24 Comparison of Theoretical And Experimental Pressure at Side Walls of Contraction
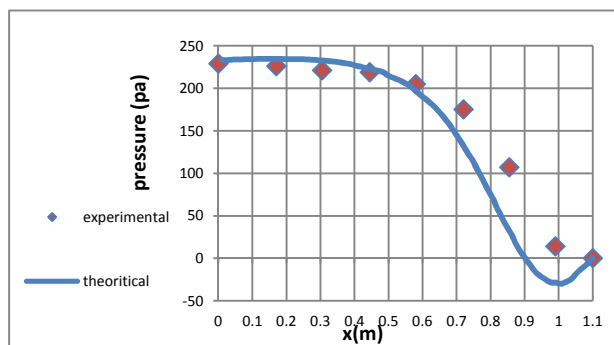
Fig.25 Comparison of Theoretical and Experimental Pressure at Top Walls of Contraction

6. CONCLUSIONS

The ANSYS workbench 15.0 with Fluent solver with k-ε turbulence model was used to design and optimize a 3-D wind-tunnel contraction section. The Matlab language was used to solve a six order polynomial equation obtained for the seven different contraction profiles. The following conclusions are obtained;

1. The high uniformity was found at the middle inflection point and when the contraction axis moves upstream.

2. No boundary layer separation takes place in all cases.

3. The boundary layer thickness at the wall of the contraction section reduces as the inflection point moves downstream the contraction axis.

4. The drop in static pressure decreases as the inflection point moves upstream the contraction axis.

5. The V-W velocities at the test section inlet were reduced as the inflection point moves upstream.

6. After estimate of these criteria, the contraction profile number four

(Xinf.=0.55) represents the thinner boundary layer thickness. The contraction profile number one (Xinf.=0.475) represents the best decreasing in the static pressure drop. The contraction profile number one (Xinf.=0.45) represents the best decreasing in the normal velocities at the test section inlet. The maximum uniformity was found at the inflection point Xinf.=0.55,also, it can be observed the minimum uniformity is obtained at the Xinf.=0.45. Based on previous results the contraction profile number four (Xinf.0.55), in which the inflection point is located at the middle of the contraction axis, was chosen to be the best profile for the present wind-tunnel.

7. The static pressure on the side and top walls decrease from upstream to downstream along the contraction axis.

8. The most uniform velocity profile is found at inlet of the test section from the seven holes on the two sides of the test sections.

9. The measurements in the center line of contraction were obtained as compared with theoretical results very well.

References

1. Abdelhamed, y.el-s. Yassen, M. Elsakka "Design Optimization Of Three Dimensional Geometry Of Wind Tunnel Contraction" mechanical engineering department, faculty of engineering, Vol.6, pp. 281–288,Egypt. (2014).

2. Ahmed d. E. and eljack E. M. "Optimization Of Model Wind Tunnel Contraction Using CFD",department of mechanical engineering, university of khartoum, Vol. 32, No.11,sudan (2014).

3. Barlow, J.B., Rae, W.H. Jr. and Pope," Low-Speed Wind Tunnel Testing", Aeronautical Journal, Department of Mechanical, Production Engineering, University of Florida, December, (1999).

4. Bradshaw and R. M. Mehta "Technical Note Design Rules For Small, Low Speed Wind Tunnels" the aeronautical journal of the royal aeronautical society, Vol. 12, pp. 443-449, (1979).

5. Downie, R. Jordinson, and F. H. Barnes" On The Design Of Three-Dimensional Wind Tunnel Contractions" Aeronautical Journal, Department of Mechanical, Production Engineering, Brighton, vol.88,No.877, pp. 287-295, (1984).

6. Mikhail, W.Rainbird, "Optimum Design Of Wind Tunnel

Contractions" 10th Aerodynamic Testing Conference, (1978).

Notation

CR: Contraction ratio

H_i: The contraction inlet height(m)

H_o: The contraction exit height(m)

A_i: The contraction inlet area (m^2)

A_o: The contraction outlet area(m^2)

L: The contraction length(m)

P: Pressure(pa)

M: Mach number

U,V,W: Velocity components in x, y and z-direction(m/s)

U_{uni}: Uniformity

X, Y, Z : Cartesian coordinates(m)

تصميم وتحسين مقطع تضييق ثلاثي الأبعاد لنفق هوائي واطئ السرعة

عقيل عاشور عبد
د. انمار حامد علي
مدرس
قسم الهندسة الميكانيكية / كلية الهندسة
جامعة بغداد

الخلاصة

في هذا البحث ، تم تصميم مقطع تضييق وتصنيعه في قسم الهندسة الميكانيكية في جامعة بغداد ـ كلية الهندسة .وقد تم إنجاز الدراسة النظرية بواسطة برنامج ANSYS 15.0 واستخدام نموذج اضطراب K-E لمحاكاة التدفق المضطرب في مقطع تضييق ثلاثي الأبعاد من نفق الرياح منخفض السرعة .وقد تم اعتماد معادلة متعددة الحدود من الدرجة السادسة بشروط حدية محددة لتمثل شكل جانبي للجدار .يتم اختيار سبع نقاط انعطاف لإعطاء سبعة تقلصات مختلفة .تم بناء نفق رياح منخفض السرعة تجريبي لمساحة المقطع العرضي للاختبار (0.45 × 0.45 متر مربع) وقسم جديد مقطع تضييق واختباره لأقصى سرعة في قسم الاختبار 20 م / ث .تعتبر سماكة طبقة الحدود والضغط الثابت والتدفق الثانوي والتماثل الأقصى كمعلمات للتحسين .تظهر النتائج العددية أن سمك الطبقة الحدودية ينخفض الى اقل ما يمكن ، زيادة في مكونات السرع العمودية للجدار في مدخل جزء الاختبار ، ويزداد احتمال فصل التدفق مع تحرك نقطة الانقلاب نحو مخرج مقطع تضييق .يتم التحقق من مقطع تضييق الأمثل بطريقة حسابية وتجريبية .المقارنة جيدة للنتائج التجريبية لمقطع تضييق مع النتائج الحسابية ANSYS 15.0 . .

الكلمات المفتاحية: ، مقطع تضييق، مقطع الاختبار ، تصميم قسم الانكماش ، نفق الرياح الصغيرة ، قسم الاختبار ، نسبة الانكماش ، تحسين قسم الانكماش ، توحيد السرعة